

Control methods for T^4 Scaling of the Fisher Information with quantum sensing

Tuvia Gefen,¹ Fedor Jelezko,² and Alex Retzker¹

¹*Racah Institute of Physics, The Hebrew University of Jerusalem, Jerusalem 91904, Givat Ram, Israel*

²*Institute for Quantum Optics, Ulm University, Albert-Einstein-Allee 11, Ulm 89081, Germany*

(Dated: December 3, 2024)

Recently new approaches for sensing time dependent Hamiltonians have been presented, and a new scaling of the Fisher information was introduced: the T^4 scaling. We present here our interpretation of this new scaling, where the relative phase is accumulated quadratically with time, and show that this can be produced by a variety of simple pulse sequences. Interestingly, this scaling has a limited duration, and we show that certain pulse sequences prolong the effect. The performance of these schemes is analyzed and we examine their relevance to state-of-the-art experiments.

PACS numbers: 03.67.Ac, 03.67.-a, 37.10.Vz, 75.10.Pq

Introduction — Quantum sensing[1–3] and metrology[4–6] utilizes individual quantum systems or collective quantum phenomena to improve measurement precision. A typical quantum sensing protocol consists of a series of signal measurements where each lasts for a duration τ . In the case of a static signal the acquired phase scales as τ , which accounts for a Fisher Information (FI) of $4\tau^2$ and thus precision of $\frac{1}{2\tau}$. A finite coherence time, due to different kinds of noise, usually lead to a precision that scales as $\frac{1}{\sqrt{TT_2}}$ [7–9], where T_2 denotes the coherence time of the probe and T is the total time. Interestingly recent theoretical and experimental works have shown that the precision behaves differently when estimating the frequency of a time dependent signal [10–12]. These studies reported that T^4 scaling of the FI is achievable and a tight upper bound was calculated in ref. [11]. Here we present our interpretation of this scaling together with a set of coherent control methods that lead to it.

T^4 scaling of the FI was first introduced in [11] and was demonstrated for the following Hamiltonian:

$$H = \Omega (\sigma_X \cos(2\omega t) + \sigma_Y \sin(2\omega t)). \quad (1)$$

The method proposed in [11] for T^4 scaling can be understood as follows. Applying stroboscopically a control of:

$$H_C = -\Omega (\sigma_X \cos(2\omega' t) + \sigma_Y \sin(2\omega' t)) + \omega' \sigma_Z, \quad (2)$$

we get the following Hamiltonian:

$$H_e = \Omega \sigma_X (\cos(2\omega t) - \cos(2\omega' t)) + \Omega \sigma_Y (\sin(2\omega t) - \sin(2\omega' t)) + \omega' \sigma_Z. \quad (3)$$

Now if ω is known to a high degree, namely $\delta t \ll 1$, where $\delta = |\omega - \omega'|$, and after moving to the interaction picture with respect to $\omega' \sigma_Z$ we get:

$$H_e \approx 2\Omega \delta t \sigma_Y. \quad (4)$$

This effective Hamiltonian leads to a FI of $4\Omega^2 t^4$ since the accumulated phase now grows as $\Omega \delta t^2$, unlike the standard scaling of δt . This method, however, requires a knowledge of Ω .

The Hamiltonian:

$$H = \Omega \sigma_Z \sin(\omega t) \quad (5)$$

was studied in ref. [10], as it was realized experimentally with NV centers in diamond. We can readily observe that a similar method also works for this case. Choosing a control Hamiltonian of:

$$H_C = -\Omega \sigma_Z \sin(\omega' t) + \frac{\pi}{2} \delta \left(t - \frac{\pi}{2\omega'} (2N+1) \right) \sigma_X, \quad (6)$$

the second term represents a decoupling sequence which is composed of fast π pulses and can be realized by an XY8 sequence or a CPMG[13, 14]. By adding the original Hamiltonian and the control we get:

$$H_e \approx \Omega \delta t \sigma_Z \cos(\omega' t) + \frac{\pi}{2} \delta \left(t - \frac{\pi}{2\omega'} (2N+1) \right) \sigma_X. \quad (7)$$

Now moving to the interaction picture with respect to the pulses we get: $H_e = \Omega \delta t \sigma_Z |\cos(\omega' t)|$, which leads to a quadratic phase accumulation. However, as it was shown in [10, 12], the first term in H_C is redundant and only pulses are required. The pulses lead to an effective Hamiltonian of:

$$H_e = \frac{2}{\pi} \Omega \sin(\delta t) \sigma_Z, \quad (8)$$

where $\delta = \omega - \omega'$, and assuming again that $\delta t \ll 1$ we get:

$$H_e = \frac{2}{\pi} \Omega \delta t \sigma_Z. \quad (9)$$

Therefore a FI of $(\frac{2}{\pi})^2 \Omega^2 t^4$ is achieved, it can be verified with the technique presented in ref. [11] that this FI is optimal. Unlike the first method this method does not require knowledge of Ω . This implies that similar pulse sequences may lead to a phase acceleration with Hamiltonians of the first kind. Both of these methods, however, do require the knowledge of the phase. In the rest of the paper we refer to the Hamiltonian in eq.1 as the first kind and to the Hamiltonian in eq.5 as the second kind.

Simple dynamical decoupling methods— Concentrating on the first kind, We claim that phase acceleration can be obtained by a dynamical decoupling method, which does not require knowledge of Ω . Adding to (Eq.1) a term of $\omega' \sigma_Z$ and moving to the interaction picture with respect to it yields:

$$H_I = \Omega (\sigma_X \cos(2\delta t) + \sigma_Y \sin(2\delta t)). \quad (10)$$

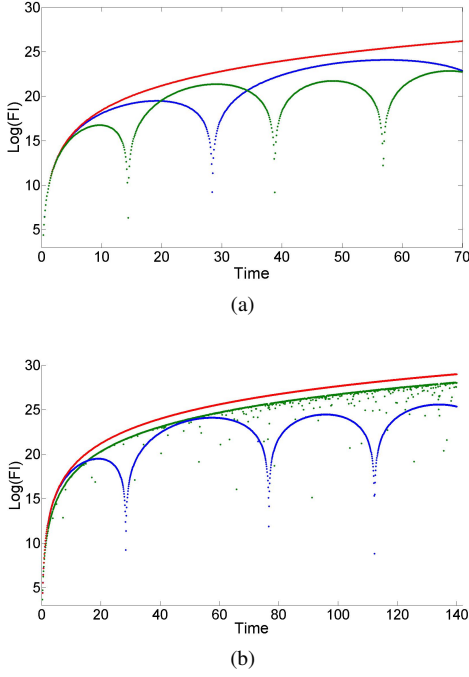


Figure 1. Top: FI achieved with the first dynamical decoupling method, compared with the optimal FI. The green curve corresponds to $\delta = 0.08\omega$, the blue to $\delta = 0.04\omega$ and the red is the optimal FI. The optimal FI coincides with this method only for $\delta t \ll 1$, as can be seen from eq. 11.

Bottom: Comparison between the two different dynamical decoupling methods. The blue curve corresponds to the first method, the green to the second and the red is the optimal FI. For short times ($\delta t \ll 1$) the first method is superior as it achieves the optimal FI. However it loses this advantage quite quickly as it suffers from a shorter lifetime. In both plots $\Omega = 50\omega$.

Applying π -pulses of σ_Y (in the interaction picture) every Δt , such that $\Omega\Delta t, \delta\Delta t \ll 1$, will transform σ_X to $-\sigma_X$ so this term will be canceled out and we will be left with: $H_{Ie} = \Omega\sigma_Y \sin(2\delta t)$. Hence a quadratic phase accumulation is achieved in the limit of $\delta t \ll 1$. We remark that this dynamical decoupling could be implemented continuously by opening a large energy gap in σ_Y direction. As reported in [10] the FI of H_{Ie} reads:

$$\frac{\Omega^2}{\delta^4} (\cos(2\delta t) - 1 + 2\delta t \sin(2\delta t))^2, \quad (11)$$

therefore in the limit of $\delta t \ll 1$ the optimal FI is achieved. Eq. 11 explicitly shows that the lifetime of the T^4 scaling goes as $\sim \frac{1}{\delta}$, and for longer times the FI becomes $4\frac{\Omega^2}{\delta^2} \sin^2(2\delta T) T^2$. This is illustrated with numerical results in fig. 1(a). It means that favorable scaling is achieved only when the frequency of the signal is known with a very good precision.

It is natural to inquire whether other dynamical decoupling methods can achieve this scaling with a longer duration.

Let us first examine why a standard scaling is achieved in the absence of control. It can be seen that the dynamics in the

slot $(0, t)$ is given by the unitary:

$$U(t) = \exp(-i\delta\sigma_Z t) \exp(-i(-\delta\sigma_Z + \Omega\sigma_X)t). \quad (12)$$

This time evolution clearly cannot lead to an improved FI as it represents the concatenation of two standard rotations. Observe that the unitary for the time slot $(t, t + \Delta t)$ reads:

$$U(t, t + \Delta t) = \exp(-i\delta\sigma_Z \Delta t) \cdot \exp(-i(-\delta\sigma_Z + \Omega \cos(2\delta t) \sigma_X + \Omega \sin(2\delta t) \sigma_Y) \Delta t). \quad (13)$$

In leading order of $\frac{\delta}{\Omega}$, where $\delta \ll \Omega$, the unitary reads:

$$U(t, t + \Delta t) = \exp(-i\delta\sigma_Z \Delta t) \cdot \exp(-i\Omega (\cos(2\delta t) \sigma_X + \sin(2\delta t) \sigma_Y) \Delta t). \quad (14)$$

Taking $\Delta t = \frac{\pi}{2\Omega}$ we get:

$$U(t, t + \Delta t) = i(\sigma_X \cos(2\delta t + \delta \Delta t) + \sigma_Y \sin(2\delta t + \delta \Delta t)). \quad (15)$$

The intuition is clear, in the limit of small $\delta\Delta t$ we expect $U(t, t + \Delta t) \approx \exp(-i\Omega (\cos(2\delta t) \sigma_X + \sin(2\delta t) \sigma_Y) \Delta t)$. Hence $U(t, t + \Delta t)$ is a rotation around $\sigma_X \cos(2\delta t + \delta \Delta t) + \sigma_Y \sin(2\delta t + \delta \Delta t)$ axis with an angle of π . The dynamics therefore can be understood as follows: in each time slot of $(t, t + \Delta t)$ our state is rotated around $\sigma_X \cos(2\delta t + \delta \Delta t) + \sigma_Y \sin(2\delta t + \delta \Delta t)$ axis with an angle of π . The axis of rotation thus rotates, unlike the static Hamiltonian case. It should be noted that this property is not manifested in the state evolution. For example the state $|\downarrow_x\rangle$ will undergo the following evolution:

$$U(t, 0) |\downarrow_x\rangle = U(N\Delta t, (N-1)\Delta t) \dots U(2\Delta t, \Delta t) U(\Delta t, 0) |\downarrow_x\rangle = \cos(\delta N \Delta t) |\downarrow_x\rangle + i \sin(\delta N \Delta t) |\uparrow_x\rangle \quad (16)$$

This adiabatic evolution is illustrated in fig. 2, showing that the state rotates with the unitaries and therefore the accumulated phase is linear with time. In fact, in each time interval the previous angle of rotation is subtracted from the new angle of rotation, and thus the phase accumulation is not optimal. Clearly, if the angles of rotations could be summed up instead of subtracted from each other, then the total acquired phase would be larger, resulting in a better FI. This indeed can be accomplished just by applying a π -pulse around the σ_x -axis (or σ_y -axis) every Δt , namely by reflecting across the σ_x -axis. The intuition behind this control is clarified in fig. 2, the angles of rotations are now summed up leading to an accelerated phase accumulation:

$$\begin{aligned} U(N\Delta t, (N-1)\Delta t) \Pi_x \dots \Pi_x U(2\Delta t, \Delta t) \Pi_x U(\Delta t, 0) |\downarrow_x\rangle \\ = \cos\left(\delta \sum_{k=1}^N (2k-1) \Delta t\right) |\downarrow_x\rangle + i \sin\left(\delta \sum_{k=1}^N (2k-1) \Delta t\right) |\uparrow_x\rangle \\ = \cos\left(\delta \frac{t^2}{\Delta t}\right) |\downarrow_x\rangle + i \sin\left(\delta \frac{t^2}{\Delta t}\right) |\uparrow_x\rangle, \end{aligned}$$

where t is the total time. The resulting FI reads: $I = 4 \left(\frac{t^2}{\Delta t}\right)^2 = 4 \frac{t^4}{(\Delta t)^2} = 4\Omega^2 t^4 \left(\frac{\pi}{2}\right)^2$ hence the accelerated phase accumulation gives rise to a t^4 scaling. Note that although optimal scaling is achieved, however the FI of this method is smaller than

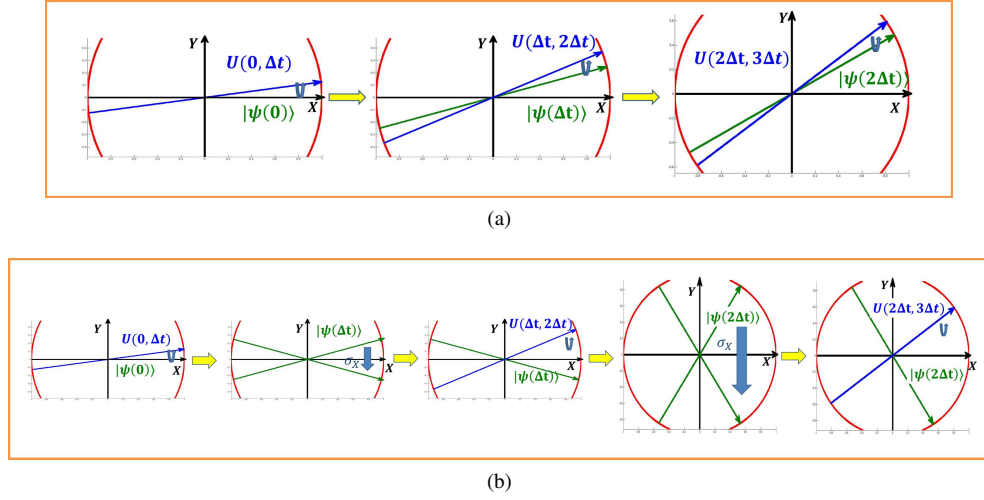


Figure 2. Illustration of the second method in Bloch sphere ($x-y$ plane). Top: Adiabatic evolution of the spin under the Hamiltonian of eq. 10. The unitary is rotated with a frequency of 2δ and the state evolves along it. The state undergoes a π -pulse with a different unitary every Δt , as $\Delta t = \frac{\pi}{2\Omega}$. However these different angles do not accumulate and it rotates with the same frequency as the unitary. Bottom: Now in addition to the unitary evolution a π -pulse around σ_x axis is applied every Δt . Due to these π -pulses the different angles are accumulated, and the rotation angle of the state goes as $\delta \frac{t^2}{\Delta t}$.

the optimal value by a prefactor of $(\frac{2}{\pi})^2$. More generally, for $\Delta t = (2k+1) \frac{\pi}{2\Omega}$ the FI reads:

$$I = 4\Omega^2 t^4 \left(\frac{2}{\pi(2k+1)} \right)^2. \quad (18)$$

The scheme works as long as our approximation of $\sqrt{\Omega^2 + \delta^2} t \approx \Omega t$, holds, which means that the duration of this method is approximately $\frac{\Omega}{\delta^2}$. This presents a significant improvement over the lifetime of the other methods ($\frac{1}{\delta}$). A comparison between the different methods is presented in figure 1(b). One more advantage, which might be experimentally important, is that the SNR (signal to noise ratio) in this method is much improved over that in other schemes. Recall that in the first method the effective Hamiltonian scaled as $\Omega \delta t$, with a limitation of $\delta t \ll 1$, while here the effective Hamiltonian scales as Ω .

The main limitation of this scheme is the need to know Ω to a high degree, so that π -pulses can be applied every $\frac{\pi}{2\Omega}$. Regarding this point, we shall examine the behavior of the FI for different timings (Δt) of the π -pulses. Clearly not every Δt leads to a T^4 scaling: Taking $\Delta t = N \frac{\pi}{\Omega}$, for an integer N , we obtain $U(t, t + \Delta t) = \exp(i\delta \sigma_Z \Delta t)$ so that phase acceleration cannot be obtained. For a general Δt the analysis becomes more tricky, some numerical results are shown in figure 3. For $\Delta t = \frac{\pi}{2\Omega}$ the probability equals to $\cos^2\left(\delta \frac{t^2}{\tau}\right)$, so the T^4 oscillations have a unit amplitude (up to small deviations that go as $\frac{\delta^2}{\Omega^2} t$). These T^4 oscillations do not disappear for different Δt , but their amplitude drops dramatically and vanishes for values of $\frac{N\pi}{\Omega}$.

We note that this analysis is also relevant for Hamiltonians of the second kind. This can be seen by moving to the interaction picture with respect to $\frac{\omega'}{2} \sigma_Y$ and neglecting the fast rotat-

ing terms, which yields: $H_I = \frac{\Omega}{2} (\sigma_Z \cos(\delta t) + \sigma_X \sin(\delta t))$. In this case the FI drops by a factor of $\frac{1}{4}$ but the lifetime is longer. Note that if the Hamiltonian in 5 is realized by applying an electromagnetic field (as described in ref. [10]), then we can obtain the desired Hamiltonian by simply changing the polarization of the field to a circular one. This can be done via a configuration which is shown in [15–19]

Unknown initial phase— Until now it was assumed that the initial phase was known, however it is not always the case in many realistic problems. This is because it is impossible to lock the control to the phase of the signal, which is usually created by an external source. We now show that an unknown phase does not change dramatically the FI. It can be easily seen that the second method yields an accelerated phase in this case as well. Given an unknown initial phase ϕ , observe that for $\Delta t = \frac{\pi}{2\Omega}$ we have $U((k+1)\Delta t, k\Delta t) = i(\sigma_x \cos((2k+1)\Delta t + \phi) + \sigma_y \sin((2k+1)\Delta t + \phi))$. Therefore the transition probability now reads $\sin\left(\delta \left(\frac{t^2}{\Delta t} + \frac{t}{\Delta t} \phi\right)\right)^2$. There is still a quadratic phase accumulation, the only difference now is the new term $\frac{t}{\Delta t} \phi$, namely the unknown phase. The FI matrix now reads:

$$I = 4\Omega^2 \left(\frac{2}{\pi}\right)^2 \begin{pmatrix} T^4 & T^3 \\ T^3 & T^2 \end{pmatrix}, \quad (19)$$

so $I_{\delta, \delta}$ is unchanged, but it is not the quantity of interest. Recall that the variance in estimating δ is now bounded by $(I^{-1})_{\delta, \delta}$, which now equals to infinity since I is not invertible. This makes sense as no information about δ can be obtained due to the unknown phase. In order to retrieve the T^4 scaling we must have identical probes that feel the same signal and they should have different measurement times. For two systems, it can be easily seen that the optimal measurement

times are: $T, 0.45T$, which yields FI of $\sim \frac{\Omega^2}{10} \left(\frac{2}{\pi}\right)^2 T^4$. Thus, T^4 scaling can be achieved, but with a prefactor of $\frac{1}{40}$ due to the unknown phase. Determining the optimal measurement times and finding tight bounds of the FI for a large number of systems is left as an open challenge.

As for the first method: the phase acceleration depends on the phase, but only phases of $\phi = \pm \frac{\pi}{2}$ ruin it completely. It can be seen explicitly: in the first dynamical decoupling method we had: $H_{Ie} = \Omega \sigma_Y \sin(2\delta t + \phi)$, so for $\delta t \ll 1$ it is just: $H_{Ie} = \Omega (2\delta t \cos(\phi) + \sin(\phi)) \sigma_Y$. Hence the phase acceleration term is multiplied by a factor of $\cos(\phi)$. A similar analysis of the FI matrix yield similar results: Optimizing over two measurement times the FI reads $\sim \frac{\Omega^2}{10} T^4 \cos(\phi)^2$. So as expected there is a factor of $\cos(\phi)^2$, and the optimization problem for the general case is the same as in the second method.

Experimental relevance — Let us discuss now the applicability of this scaling. This scaling presents a clear advantage over the standard T^2 scaling as long as $\Omega T > 1$, with an improvement of a factor of $(\Omega T)^2$. However, since the analysis did not take the effect of noise into account, the finite coherence time of the probe and the signal were neglected. Let $T_\phi(\tau)$ denote the coherence time of the signal (probe). For a variety of probes, including NV centers, τ is basically T_2 . If $T_\phi \leq \tau$, it is easy to see that we gain an improvement by a factor of $(\Omega T_\phi)^2$.

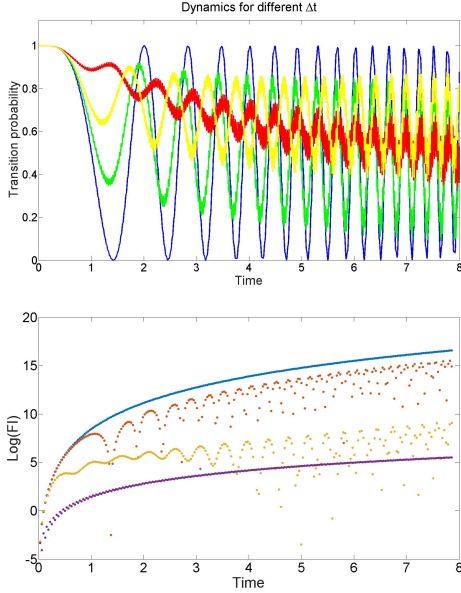


Figure 3. Numerical analysis of the FI behavior under different timings of π -pulses. Top: dynamics of transition probability for different timings, where $\Delta t = \frac{\pi}{20}$ (blue), $\frac{\pi}{96}$ (green), $\frac{\pi}{9}$ (red), $\frac{\pi}{2.06}$ (yellow). It can be seen that for $\Delta t = \frac{\pi}{20}$ perfect T^4 oscillations are achieved, while for other values the amplitude drops significantly. Bottom: comparison of the FI for different timings: $\Delta t = \frac{\pi}{20}$ (blue), $\frac{\pi}{96}$ (orange), $\frac{\pi}{9}$ (yellow) and no control (purple).

In the other regime in which the coherence time of the probe is much shorter than the coherence time of the signal, namely $\tau \ll T_\phi \approx T$, where T is the total time, the behavior of the FI is less trivial. The first observation regarding this regime is that in the absence of any coherent control, the FI scales as T^3 . Let us show this for the Hamiltonian of the first kind. The QFI of a single measurement performed in a period of $(t, t + \tau)$ is bounded by $4(t + \tau)^2$. This bound is almost achieved for $\tau = (2N + 1) \frac{\pi}{2\Omega}$, for which the FI is $(2t + \tau)^2$. Hence assuming τ takes one of these values the total FI reads:

$$I_{tot} = \sum_k I_k = \sum_k (2k + 1)^2 \tau^2 \approx 4 \frac{T^3}{3\tau} \leq \frac{8}{3\pi} \Omega T^3, \quad (20)$$

thus a T^3 scaling is achieved. Without coherent control the optimal τ is again $\frac{\pi}{2\Omega}$, this suggests that for larger τ coherent control may be useful. Recall that with coherent control an effective Hamiltonian: $H_e = 2\Omega\delta t \sigma_Y$ can be obtained. In this case the FI for the interval $(t, t + \tau)$ is $4\Omega^2 \left((t + \tau)^2 - t^2 \right)^2$, and the total FI reads:

$$I_{tot} = \sum_k I_k = \sum_k 4\Omega^2 \left((k + 1)^2 - (k)^2 \right)^2 \tau^4 \approx \frac{16}{3} (\Omega^2 \tau) T^3, \quad (21)$$

where, again, $\tau \leq T_2$. This again yields a T^3 scaling, but as expected there is an improvement by a factor of the order of $\Omega\tau$.

The picture is a bit different for the Hamiltonian $H = \Omega \sigma_Z \sin(2\omega t)$. We know that by applying the appropriate control the frequency ω is changed to δ and for $\delta T \ll 1$, a T^4 scaling is achieved. Therefore, let us focus on $H = \Omega \sigma_Z \sin(2\delta t)$, and examine how the FI changes as a function of δ for a given single experiment time of τ . The total FI reads:

$$I_{tot} = \sum_k I_k = \frac{\Omega^2}{\delta^4} \cdot \sum_k \left(2\delta t_k \sin(2\delta t_k) - 2\delta t_{k+1} \sin(2\delta t_{k+1}) + \cos(2\delta t_k) - \cos(2\delta t_{k+1}) \right)^2. \quad (22)$$

It can be seen that for $\delta\tau \ll 1$ the FI is given by:

$$I_{tot} = 16\Omega^2 \tau \left(\frac{T^3}{6} + \frac{T \cos(4\delta T)}{16\delta^2} + \frac{(8\delta^2 T^2 - 1) \sin(4\delta T)}{64\delta^3} \right). \quad (23)$$

Hence for $\delta T \ll 1$ we get $\frac{16}{3} \Omega^2 \tau T^3$, which is limited by $\frac{16}{3} \Omega^2 T_2 T^3$. In the regime where δT is no longer small but still $\delta\tau \ll 1$, the FI drops by a factor of 2 to $\frac{16}{6} \Omega^2 \tau T^3$. This is just due to the factor of $\cos^2(\phi)$ that is added in an arbitrary phase ϕ . Now for larger δ , where $\delta\tau$ is no longer small, the FI to a good approximation reads:

$$I_{tot} = 4 \left(\frac{\Omega}{\delta} \right)^2 \frac{T^3}{3\tau} (1 - \cos(2\delta\tau)). \quad (24)$$

Note that if $\delta\tau$ is too large it is no longer optimal to perform a measurement every τ , and shorter measurement periods are

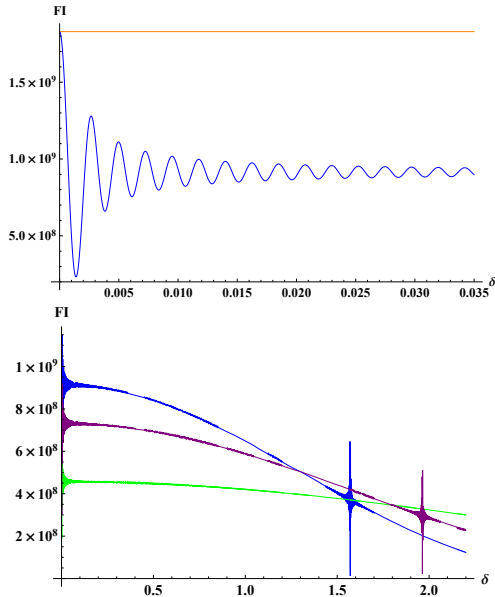


Figure 4. Analysis of the FI as a function of time for a given measurement period τ . Top: Behavior of the FI in the regime of $\delta\tau \ll 1$. Observe that the FI coincides with the ultimate limit (orange curve) for $\delta\tau \ll 1$ and then oscillates and drops to half of this limit. Bottom: The FI for larger δ and different values of τ : 1 (blue), 0.8 (purple), 0.5 (green), $\frac{1}{3}$ (red). The FI goes as $I_{\text{tot}} = 4 \left(\frac{\Omega}{\delta}\right)^2 \frac{T^3}{3\tau} (1 - \cos(2\delta\tau))$, this serves as a good approximation except for $\delta = 0, \frac{\pi}{2\delta}$ in which there are sharp oscillations. τ is the optimal measurement period only for $\delta < \frac{1.165}{\tau}$.

preferable. It turns out that τ is optimal as long as $\delta < \frac{1.165}{\tau}$, and for larger δ the optimal measurement period is $\frac{1.165}{\delta}$, as shown in fig. 4. Plugging this into eq. 24, we get:

$$I_{\text{tot}} \approx 1.93 \frac{\Omega^2}{\delta} T^3, \quad (25)$$

therefore in this regime, if the measurement period is chosen wisely the FI drops as $\frac{1}{\delta}$.

Conclusions and outlook— This paper describes novel schemes designed to achieve T^4 scaling of the FI. A detailed analysis of the schemes demonstrated that they function for extended times. As the proposed T^4 methods are adaptive the extension of time is crucial for experimental realization. We anticipate that the use of these schemes will find applications in nano imaging and in atomic clocks protocols. It is still an open question as to whether T^4 scaling can be reached in a non adaptive way. It is noteworthy that the resolution of the T^4 method scales with $(\Omega T_2)^2$, meaning that it improves quadratically with the strength of the signal.

Acknowledgements — A. R. acknowledges the support of the Israel Science Foundation (grant no. 1500/13), the support of the European commission (STReP EQUAM Grant Agreement No. 323714), EU Project DIADAMS, the Marie Curie Career Integration Grant (CIG) IonQuanSense(321798), the Niedersachsen-Israeli Research Cooperation Program and DIP program (FO 703/2-1). This project has received funding from the European Union Horizon 2020 (Hyperdiamond).

-
- [1] C. L. Degen, F. Reinhard, and P. Cappellaro. Quantum sensing. *arXiv preprint arXiv:1611.02427*, 2016.
 - [2] Dmitry Budker and Michael Romalis. Optical magnetometry. *Nature Physics*, 3(4):227–234, 2007.
 - [3] L Rondin, JP Tetienne, T Hingant, JF Roch, P Maletinsky, and V Jacques. Magnetometry with nitrogen-vacancy defects in diamond. *Reports on progress in physics*, 77(5):056503, 2014.
 - [4] JJ Bollinger, Wayne M Itano, DJ Wineland, and DJ Heinzen. Optimal frequency measurements with maximally correlated states. *Physical Review A*, 54(6):R4649, 1996.
 - [5] Vittorio Giovannetti, Seth Lloyd, and Lorenzo Maccone. Quantum-enhanced measurements: beating the standard quantum limit. *Science*, 306(5700):1330–1336, 2004.
 - [6] Vittorio Giovannetti, Seth Lloyd, and Lorenzo Maccone. Quantum metrology. *Physical review letters*, 96(1):010401, 2006.
 - [7] WM Itano, JC Bergquist, JJ Bollinger, JM Gilligan, DJ Heinzen, FL Moore, MG Raizen, and DJ Wineland. Quantum projection noise: Population fluctuations in two-level systems. *Physical Review A*, 47(5):3554, 1993.
 - [8] Carl W Helstrom. Quantum detection and estimation theory. *Journal of Statistical Physics*, 1(2):231–252, 1969.
 - [9] Alexander S Holevo. *Probabilistic and statistical aspects of quantum theory*, volume 1. Springer Science & Business Media, 2011.
 - [10] S Schmitt, T Gefen, F Strumer, T Uden, G Wolff, C Muller, J Scheuer, B Naydenov, M Markham, S Pezzagna, J Meijer, Ilai Schwarz, M Plenio, A Retzker, and F Jelezko. Sub-milliherz magnetic spectroscopy with a nanoscale quantum sensor. *unpublished*, 2016.
 - [11] Shengshi Pang, and Andrew N Jordan. Quantum metrology with time-dependent hamiltonians. *arXiv preprint arXiv:1606.02166*, 2016.
 - [12] Jing Yang, Shengshi Pang, and Andrew N Jordan. Quantum parameter estimation with the Landau-Zener transition. *arXiv preprint arXiv:1612.02390*, 2016.
 - [13] Charles P Slichter. *Principles of magnetic resonance*, volume 1. Springer Science & Business Media, 2013.
 - [14] Ray Freeman. *Spin choreography*. Oxford University Press Oxford, UK, 1998.
 - [15] Li, Z. F., Mutlu, M. and Ozbay, E. Highly asymmetric transmission of linearly polarized waves realized with a multilayered structure including chiral metamaterials. *J. Phys. D Appl. Phys.* **47**, 075107 (2014).
 - [16] Liu, D. Y., Li, M. H., Zhai, X. M., Yao, L. F. and Dong, J. F. Enhanced asymmetric transmission due to Fabry-Perot-like cavity. *Opt. Express* **22**, 11707 (2014).
 - [17] Song, K., Liu, Y., Luo, C. and Zhao, X. High-efficiency broadband and multiband cross-polarization conversion using chiral metamaterial. *J. Phys. D Appl. Phys.* **47**, 505104 (2014).
 - [18] Zhancheng Li, Wenwei Liu, Hua Cheng, Shuqi Chen and

Jianguo Tian. Realizing Broadband and Invertible Linear-to-circular Polarization Converter with Ultrathin Singlelayer

Metasurface. Scientific reports **5** 18106 (2014).
[19] Arthur Frank Harvey. Microwave engineering. 1963. (p.192).